ELSEVIER

Journal of Organometallic Chemistry 495 (1995) 61–69

Journal of Organometallic Chemistry

Synthesis and reactivity investigation of iridium maleonitriledithiolate complexes. Redox studies and extended Hückel molecular orbital calculations on $Cp^*IrL(mnt)$ (where $L = PMe_3$, PPh_3, CN-t-Bu)

K. Yang, M.-J. Don, D.K. Sharma, S.G. Bott *, M.G. Richmond *

Center for Organometallic Research and Education, Department of Chemistry, University of North Texas, Denton, TX 76203, USA

Received 9 September 1994; in revised form 2 December 1994

Abstract

The reaction between the cyclopentadienyliridium complexes $Cp^*Ir(L)Cl_2$ (where $L = PMe_3$, PPh_3, CN-t-Bu) and disodium maleonitriledithiolate (Na_2mnt) yields the corresponding mnt-substituted compounds $Cp^*Ir(PMe_3)(mnt)$ (**1**), $Cp^*Ir(PPh_3)(mnt)$ (**2**) and $Cp^*Ir(CN\text{-}t\text{-}Bu)(mnt)$ (**3**). All of these new compounds have been isolated in high yield and characterized in solution by IR and NMR spectroscopy. The solid state structures of **2** and **3** were determined by single-crystal X-ray diffraction analysis. **2** crystallizes in the triclinic space group $P\bar{1}$ with $a = 10.4557(8)$ Å, $b = 10.630(1)$ Å, $c = 14.894(1)$ Å, $\alpha = 91.382(8)°$, $\beta = 90.141(6)°$, $\gamma = 118.182(7)°$, $V = 1458.5(3)$ Å^3 and $Z = 2$. Full-matrix least-squares refinement yielded $R = 0.0281$ for 3425 ($I > 3\sigma(I)$) reflections. **3** crystallizes in the monoclinic space group $P2_1/n$ with $a = 8.9609(7)$ Å, $b = 20.343(1)$ Å, $c = 11.9115(9)$ Å, $\beta = 94.168(6)°$, $V = 2165.6(3)$ Å^3 and $Z = 4$. Full-matrix least-squares refinement yielded $R = 0.0245$ for 2266 ($I > 3\sigma(I)$) reflections. The redox properties of **1–3** have been explored by cyclic and rotating disc electrode voltammetric techniques in MeCN and CH_2Cl_2 solvents. Each of these compounds exhibit a well-defined one-electron oxidation wave that is assigned to the $0/+1$ redox couple, along with a $+1/+2$ redox wave, the reversibility of which is highly dependent on the nature of the ancillary two-electron donor ligand (L) and the solvent. Extended Hückel calculations have been performed on the model compounds $CpIr(PH_3)(mnt)$ and $CpIr(CNH)(mnt)$, with the results used in a discussion of the nature of the HOMO and LUMO levels in **1–3**.

Keywords: Iridium; Hückel molecular orbital calculations; Electrochemistry; Maleonitriledithiolate complexes; Cyclopentadienyl derivatives

1. Introduction

The maleonitriledithiolate ligand (mnt) has been widely used in the construction of novel organometallic compounds [1–3]. Reports of multiple redox states [4–6] and the novel conductivity properties found in selected mnt-substituted compounds [7] account, in part, for the continued interest in the synthesis and exploration of such compounds [8].

Of the many different types of mnt-substituted compounds presently known, the subclass of cyclopentadienyl-substituted mnt compounds still continues to receive attention [9–16]. However, examples of compounds possessing an ancillary pentamethylcyclopentadienyl (Cp^*) ligand are less common [17]. With this in mind, we have been interested in the preparation and redox examination of Cp^*-substituted dithiolate compounds based on the transition metals from Groups 8–10. Recent work from these labs has dealt with the dithiolate systems $Cp^*Ru(NO)(mnt)$ [18] and $Cp^*Ru(NO)(tdas)$ [19]. Accordingly, we have embarked on a study of isolobal relatives of the $Cp^*Ru(NO)$ fragment in the hopes of preparing new and unusual mnt-substituted compounds.

Here we report on the synthesis and characterization of a series of iridium compounds having the formula $Cp^*IrL(mnt)$. Included in our work are the redox properties of **1–3**, the X-ray diffraction structures of **2** and **3**, and extended Hückel MO calculations on the related model compounds $CpIr(PH_3)(mnt)$ and $CpIr(CNH)(mnt)$.

* Corresponding authors.

SSDI 0022-328X(94)05385-5

2. Results and discussion

2.1. Synthesis and solution characterization of $Cp^*IrL(mnt)$

All three of the new mnt-substituted complexes **1–3** were prepared from the requisite dichloride complex $Cp^*Ir(L)Cl_2$ [20] and a slight excess of disodium maleonitriledithiolate [21] in EtOH at 45 °C, as shown in Eq. (1). Isolation of the pure products, which ranged from red to purple in colour, was achieved by chromatography over silica gel using CH_2Cl_2 as an eluent. Typically, the yields of **1–3** were of the order of 75–85%.

Compounds **1–3** were characterized in solution by IR and NMR (^1H and ^{13}C) spectroscopies. The IR spectra of **1–3** exhibit two νCN stretches at ca. 2211 (m) and 2200 (s) cm^{-1}, which are ascribed to the vibrationally coupled asymmetric and symmetric C≡N stretches of the coordinated mnt ligand [22], with **3** possessing an intense isonitrile stretch at 2179 (vs) cm^{-1}. The NMR data for **1–3** are summarized in Table 1. Of interest is the relative frequency insensitivity of the ^{13}C chemical shifts of the mnt nitrile and olefinic carbons. From Table 1 it is seen that the ^{13}C resonances for the nitrile carbons and the mnt alkene carbons appear at ca. δ117 and 123, respectively. These chemical shift assignments have been made on the basis of the reported chemical shifts of related compounds [18,23]

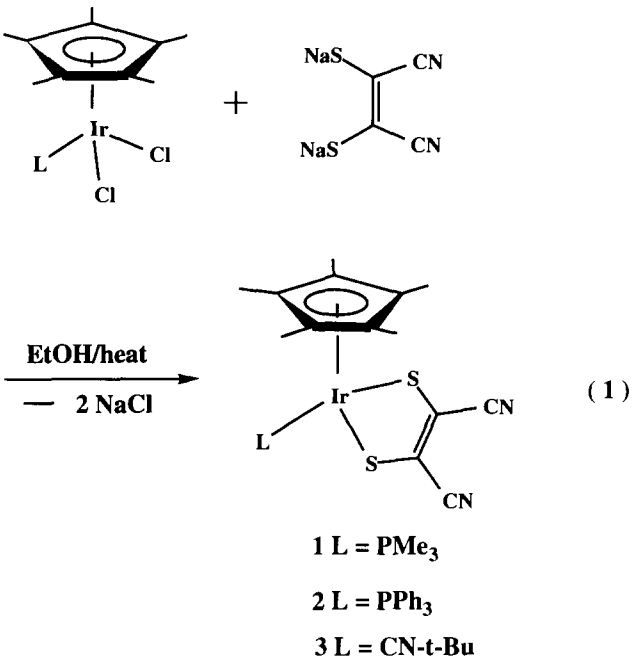

(1)

2.2. X-ray diffraction structures of $Cp^*Ir(PPh_3)(mnt)$ and $Cp^*Ir(CN\text{-}t\text{-}Bu)(mnt)$

The molecular structures of **2** and **3** were determined by X-ray diffraction analysis. Both compounds exist as discrete molecules in the unit cell with no unusually short inter- or intramolecular contacts. Table 2 lists the

Table 1
NMR spectroscopic data for compounds **1–3**

Compound	NMR (δ) [a]	
	^1H	^{13}C
1	1.47 (*d*, J_{P-H} = 10.6 Hz, PMe_3)	8.71 (Me, Cp^*)
	1.73 (*d*, J_{P-H} = 2.2 Hz, Cp^*)	13.72 (*d*, J_{P-C} = 42.3 Hz, PMe_3)
		96.94 (*d*, J_{P-C} = 3.6 Hz, Cp^* ring)
		117.21 (CN) [b]
		122.98 (mnt C=C) [b]
2	1.42 (*d*, J_{P-H} = 2.1 Hz, Cp^*)	8.26 (Me, Cp^*)
	7.42 (broad, PPh_3)	98.01 (*d*, J_{P-C} = 3.3 Hz, Cp^* ring)
		116.91 (CN) [b]
		122.93 (mnt C≡C) [b]
		127.83 (*d*, J_{P-C} = 10.3 Hz, *ortho* Ph) [c]
		129.97 (*d*, J_{P-C} = 56.6 Hz, P–C Ph)
		130.76 (*para* Ph)
		134.68 (*d*, J_{P-C} = 8.9 Hz, *meta* Ph) [c]
3	1.46 (Me, t-Bu group)	8.65 (Me, Cp^*)
	1.81 (Cp^* ring)	31.03 (Me, t-Bu group)
		58.49 (C, t-Bu group)
		97.72 (Cp^* ring)
		116.83 (CN) [b]
		123.22 (mnt C=C) [b]

[a] All NMR spectra were recorded in $CDCl_3$ at room temperature
[b] These mnt resonances may be reversed
[c] These aryl resonances may be reversed

Table 2
X-ray crystallographic data and processing parameters for compounds **2** and **3**

	2	**3**
Space group	$P\bar{1}$, triclinic	$P2_1/n$, monoclinic
a (Å)	10.4557(8)	8.9609(7)
b (Å)	10.630(1)	20.343(1)
c (Å)	14.894(1)	11.9115(9)
α (deg)	91.382(8)	
β (deg)	90.141(6)	94.168(6)
γ (deg)	118.182(7)	
V (Å^3)	1468.5(3)	2165.6(3)
Mol. formula	$C_{32}H_{30}IrN_2PS_2$	$C_{19}H_{24}IrN_3S_2$
fw	729.81	550.75
Formula units per cell (Z)	2	4
ρ (g cm^{-3})	1.662	1.689
Abs. coeff. (μ) (cm^{-1})	47.74	63.33
λ (MoK$_\alpha$) (Å)	0.71073	0.71073
Collection range (deg)	$2.0 \le 2\theta \le 44.0$	$2.0 \le 2\theta \le 44.0$
Max. scan time (s)	120	120
Scan speed range (deg min^{-1})	0.67–8.0	0.67–8.0
Total no. of data collected	3560	2933
No. of independent data ($I > 3\sigma(I)$)	3425	2266
R	0.0281	0.0245
R_w	0.0318	0.0279
Weights	$[0.04F^2 + (\sigma F^2)^2]^{-1}$	$[0.04F^2 + (\sigma F)^2]^{-1}$

X-ray data collection and processing parameters, while Tables 3 and 4 give the atomic coordinates and selected distances and angles, respectively.

Fig. 1 shows the ORTEP diagrams of **2** and **3** and confirms the six-coordinate geometry about each iridium centre, assuming that the Cp* ligand functions as a three-coordinate ligand. Each compound possesses idealized C_s molecular symmetry, as is typically found in many three-legged piano stool complexes. Both **2** and **3** have similar Ir–S bond lengths of 2.346 Å (ave.) and 2.351 Å (ave.), respectively, in good agreement with the existing values in the literature for a wide variety of Ir–S sigma bonds [8e,24]. The distance for the Ir–C(21) isonitrile bond of 1.931(8) Å and the nearly linear Ir–C(21)–N(21) bond angle of 175.9(8)° in **3** agree well with analogous lengths and angles reported for other iridium isonitrile complexes [25]. In each structure the iridium centre is perpendicular to the plane defined by the Cp* ring. The bond lengths and angles associated with the Cp* and coordinated-mnt ligands in **2** and **3** are unexceptional with respect to other mnt-substituted compounds.

2.3. Electrochemical studies on compounds 1–3

All cyclic voltammetry studies were conducted at a platinum electrode in CH_2Cl_2 and MeCN, which contained 0.2 M tetra-butylammonium perchlorate (TBAP) as the supporting electrolyte. The pertinent electrochemistry data are summarized in Table 5.

Both phosphine-substituted compounds displayed two redox responses, which are assigned to the $0/+1$ and $+1/+2$ redox couples. Fig. 2(a) shows the cyclic voltammogram for **1** in MeCN solvent. The well-defined $0/+1$ redox couple in **1** and **2** can be regarded as a fully reversible, diffusion-controlled process on the basis of the peak current (I_{p^c}/I_{p^a}) ratios of unity and plots of the current function (I_p) vs. the square root of the scan rate (ν), which were linear over the scan rate range of 0.1–1.0 V s^{-1} [26]. The one-electron nature of

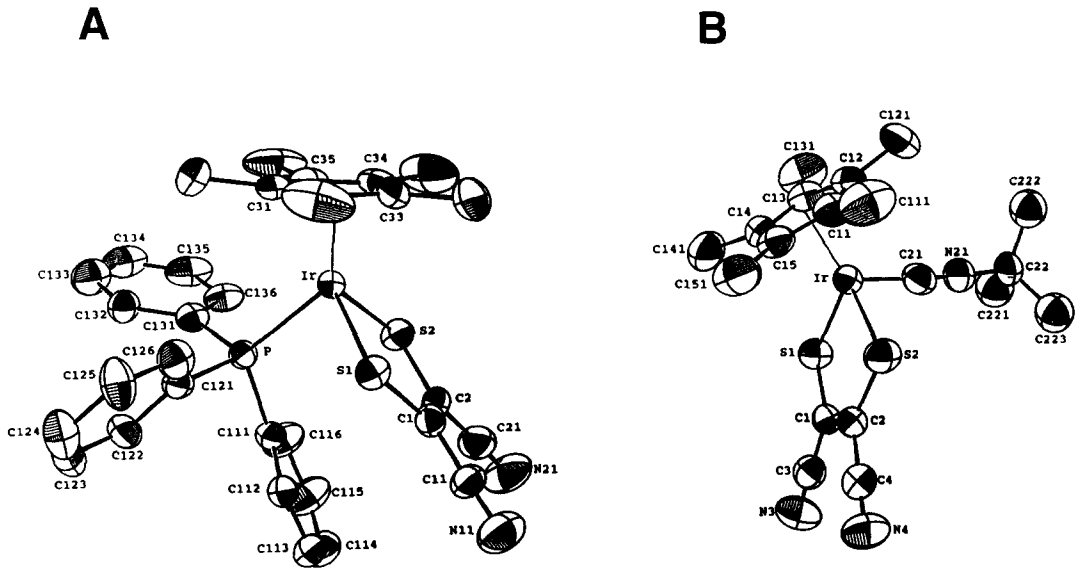

Fig. 1. ORTEP drawings of the non-hydrogen atoms of (a) Cp* Ir(PPh$_3$)(mnt) and (b) Cp* Ir(CN-t-Bu)(mnt). Thermal ellipsoids are drawn at the 50% probability level.

Table 3
Positional parameters of the non-hydrogen atoms for compounds **2** and **3** with estimated standard deviations in parentheses [a]

Atom	x	y	z	B (Å²)
Cp* Ir(PPh$_3$)(mnt) (**2**)				
Ir	0.51083(2)	0.17712(2)	0.23107(2)	2.296(5)
S(1)	0.4734(1)	−0.0285(2)	0.1489(1)	2.94(3)
S(2)	0.4693(1)	0.0462(2)	0.3624(1)	3.30(4)
P	0.7537(1)	0.2424(2)	0.2402(1)	2.53(3)
N(11)	0.3776(6)	−0.4037(7)	0.1727(6)	5.4(2)
N(21)	0.3956(7)	−0.3106(7)	0.4382(6)	6.4(2)
C(1)	0.4350(5)	−0.1544(6)	0.2322(5)	2.9(1)
C(2)	0.4386(5)	−0.1195(6)	0.3213(5)	3.0(1)
C(11)	0.4045(5)	−0.2924(6)	0.2012(6)	3.5(2)
C(21)	0.4136(6)	−0.2259(7)	0.3864(6)	4.3(2)
C(31)	0.5181(5)	0.3695(6)	0.1704(6)	4.0(2)
C(32)	0.4064(5)	0.2460(7)	0.1266(6)	4.1(2)
C(33)	0.3009(5)	0.1711(7)	0.1908(6)	3.8(2)
C(34)	0.3453(5)	0.2460(6)	0.2737(5)	4.2(1)
C(35)	0.4799(5)	0.3661(6)	0.2618(6)	3.9(2)
C(111)	0.7949(5)	0.1113(6)	0.2937(5)	3.0(1)
C(112)	0.7908(5)	0.0004(7)	0.2426(6)	3.8(2)
C(113)	0.8073(6)	−0.1079(7)	0.2823(7)	4.7(2)
C(114)	0.8307(7)	−0.1028(7)	0.3730(7)	5.6(2)
C(115)	0.8377(8)	0.0061(9)	0.4229(7)	6.1(2)
C(116)	0.8203(7)	0.1154(7)	0.3848(6)	4.9(2)
C(121)	0.8502(5)	0.2668(6)	0.1352(5)	2.8(1)
C(122)	0.9964(5)	0.2980(7)	0.1371(6)	3.7(2)
C(123)	1.0719(5)	0.3199(7)	0.0591(6)	4.0(2)
C(124)	1.0046(6)	0.3103(9)	−0.0220(6)	4.4(2)
C(125)	0.8621(6)	0.2793(9)	−0.0250(5)	4.2(2)
C(126)	0.7856(5)	0.2577(7)	0.0534(5)	3.4(2)
C(131)	0.8596(5)	0.4120(6)	0.3008(5)	2.9(1)
C(132)	0.9715(6)	0.5290(7)	0.2623(6)	3.7(2)
C(133)	1.0451(7)	0.6568(8)	0.3083(7)	4.8(2)
C(134)	1.0092(7)	0.6683(8)	0.3955(7)	5.5(2)
C(135)	0.8980(7)	0.5552(8)	0.4360(6)	5.0(2)
C(136)	0.8211(6)	0.4272(7)	0.3881(6)	3.8(2)
C(311)	0.6414(7)	0.4880(8)	0.1254(9)	7.0(3)
C(321)	0.3911(7)	0.2067(9)	0.0287(7)	6.8(2)
C(331)	0.1600(7)	0.0338(9)	0.1727(9)	7.2(3)
C(341)	0.2607(8)	0.208(1)	0.3599(8)	8.7(2)
C(351)	0.5581(7)	0.4852(8)	0.3299(8)	7.8(2)
Cp* Ir(CN-t-Bu)(mnt) (**3**)				
Ir	0.09224(3)	0.18092(1)	0.05704(2)	3.530(6)
S(1)	0.0284(2)	0.1577(1)	−0.1338(2)	4.38(4)
S(2)	0.3315(2)	0.1382(1)	0.0331(2)	4.80(5)
N(3)	0.1832(9)	0.0728(4)	−0.3762(6)	7.1(2)
N(4)	0.5306(8)	0.0380(4)	−0.1666(7)	6.9(2)
N(21)	0.1786(8)	0.3222(3)	−0.0024(6)	5.6(2)
C(1)	0.1869(8)	0.1149(3)	−0.1721(6)	3.7(2)
C(2)	0.3103(8)	0.1056(4)	−0.1019(6)	3.9(2)
C(3)	0.1832(9)	0.0906(4)	−0.2861(7)	4.7(2)
C(4)	0.4320(9)	0.0676(4)	−0.1383(7)	4.6(2)
C(11)	0.1019(9)	0.1539(5)	0.2353(6)	4.9(2)
C(12)	0.0087(8)	0.2117(4)	0.2185(6)	4.4(2)
C(13)	−0.1145(8)	0.1947(4)	0.1441(6)	4.3(2)
C(14)	−0.1055(8)	0.1250(4)	0.1185(6)	4.3(2)
C(15)	0.0266(9)	0.1007(4)	0.1728(6)	4.6(2)
C(21)	0.1503(9)	0.2688(4)	0.0169(7)	4.9(2)
C(22)	0.216(1)	0.3902(4)	−0.0221(7)	5.0(2)
C(111)	0.240(1)	0.1465(7)	0.3137(8)	8.6(3)
C(121)	0.040(1)	0.2761(5)	0.2752(8)	7.7(3)
C(131)	−0.246(1)	0.2390(5)	0.1118(9)	7.5(3)
C(141)	−0.222(1)	0.0880(6)	0.0498(8)	7.4(3)
C(151)	0.077(1)	0.0306(5)	0.1745(9)	7.6(3)

Table 3 (continued)

Atom	x	y	z	B (Å²)
C(221)	0.129(2)	0.413(1)	−0.129(2)	7.3(5) *
C(222)	0.189(2)	0.429(1)	0.083(2)	6.6(5) *
C(223)	0.393(2)	0.387(1)	−0.044(2)	6.6(4) *
C(224)	0.093(4)	0.429(2)	0.031(3)	5.4(8) *
C(225)	0.185(3)	0.398(2)	−0.159(3)	4.4(6) *
C(226)	0.375(5)	0.405(2)	0.019(3)	6.9(9) *
C(227)	0.071(4)	0.422(2)	−0.081(3)	5.6(8) *
C(228)	0.270(4)	0.421(2)	0.099(7)	5.0(7) *
C(229)	0.345(4)	0.396(2)	−0.090(3)	6.2(8) *

[a] Starred atoms were refined isotropically. Anisotropically refined atoms are given in the form of the isotropic equivalent displacement parameter defined as: $(4/3)[a^2B(1,1) + b^2B(2,2) + c^2B(3,3) + ab(\cos\gamma)B(1,2) + ac(\cos\beta)B(1,3) + bc(\cos\alpha)B(2,3)$

the oxidation in these compounds was also demonstrated by calibration of the peak current (I_{p_a}) against $[Cp_2Co][PF_6]$ and rotating disc electrode (RDE) voltam-

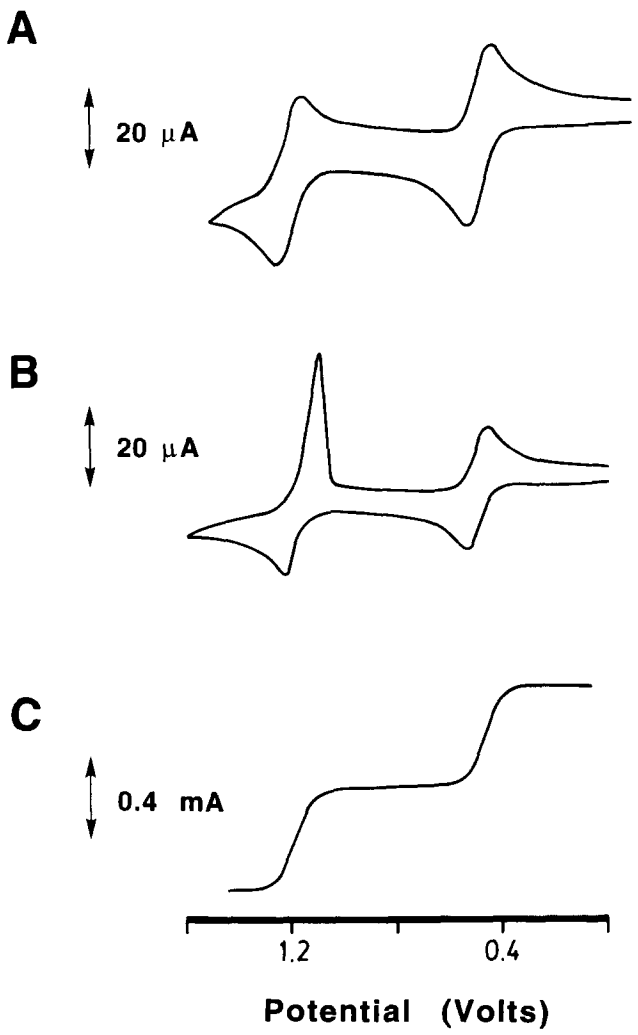

Fig. 2. Anodic scan cyclic voltammograms of ca. 1×10^{-3} M Cp* Ir(PMe$_3$)(mnt) at room temperature containing 0.2 M TBAP at 0.5 V s^{-1} in (a) MeCN and (b) CH_2Cl_2, and (c) rotating disc electrode voltammogram of ca. 1×10^{-3} M Cp* Ir(PMe$_3$)(mnt) at room temperature in MeCN containing 0.25 M TBAP at 0.05 V s^{-1}.

metry (vide infra). Analogous behaviour for the $0/+1$ redox couple in CH_2Cl_2 solvent was observed.

The second oxidation step in **1** and **2** is highly dependent on the nature of the solvent, as the $+1/+2$ redox couple is best considered as quasi-reversible in MeCN solvent, on the basis of current ratios of the order of 0.90 at 0.5 V s^{-1}. By comparison, the same redox couple is completely irreversible in CH_2Cl_2, as evidenced by the absence of a well-defined reverse couple. In the case of **1**, there is an irreversible adsorption of the transient dication $[Cp^*Ir(PMe_3)(mnt)]^{2+}$ on the platinum electrode. The initial scan cyclic voltammogram of **1** in CH_2Cl_2 showing this adsorption can be seen in Fig. 2(b).

The isonitrile-substituted compound **3** exhibits a reversible $0/+1$ redox couple in both of the solvents examined ($E_{1/2} \sim 0.55$ V), which suggests that the resulting one-electron oxidation product is similar in this family of compounds. However, a major difference that does exist between **3** and the phosphine-substituted compounds **1** and **2** is the presence of two irreversible oxidation waves at $E_{p^a} \sim 1.23$ V and $E_{p^a} \sim 1.37$ V. Increased scan rates (5 V s^{-1}) and lowered temperatures did not lead to any significant improvement in the

Table 4
Selected bond distances (Å) and angles (deg) in $Cp^*Ir(PPh_3)(mnt)$ and $Cp^*Ir(CN\text{-}t\text{-}Bu)(mnt)$ [a]

$Cp^*Ir(PPh_3)(mnt)$ (**2**)			
Bond distances			
Ir–S(1)	2.343(2)	Ir–S(2)	2.349(2)
Ir–P	2.298(1)	Ir–C(31)	2.224(7)
Ir–C(32)	2.226(8)	Ir–C(33)	2.245(6)
Ir–C(34)	2.262(7)	Ir–C(35)	2.218(7)
S(1)–C(1)	1.752(7)	S(2)–C(2)	1.730(7)
P–C(111)	1.839(7)	P–C(121)	1.819(7)
P–C(131)	1.822(6)	N(11)–C(11)	1.15(1)
N(21)–C(21)	1.15(1)	C(1)–C(2)	1.36(1)
C(1)–C(11)	1.411(9)	C(2)–C(21)	1.44(1)
C(31)–C(32)	1.421(8)	C(31)–C(35)	1.42(1)
C(32)–C(33)	1.406(9)	C(33)–C(34)	1.41(1)
C(34)–C(35)	1.399(6)	Ir–Cp^* (centroid)	1.886(7)
Bond angles			
S(1)–Ir–S(2)	88.20(6)	S(1)–Ir–P	88.85 (5)
S(2)–Ir–P	90.33(6)	Ir–S(1)–C(1)	103.1(2)
Ir–S(2)–C(2)	102.5(3)	S(1)–C(1)–C(2)	121.9(5)
S(1)–C(1)–C(11)	115.6(6)	C(2)–C(1)–C(11)	122.6(7)
S(2)–C(2)–C(1)	124.2(5)	S(2)–C(2)–C(21)	116.7(6)
C(1)–C(2)–C(21)	119.0(6)	N(11)–C(11)–C(1)	177.2(9)
N(21)–C(21)–C(2)	179.0(8)		
$Cp^*Ir(CN\text{-}t\text{-}Bu)(mnt)$ (**3**)			
Bond distances			
Ir–S(1)	2.352(2)	Ir–S(2)	2.350(2)
Ir–C(11)	2.189(7)	Ir–C(12)	2.205(8)
Ir–C(13)	2.206(7)	Ir–C(14)	2.271(8)
Ir–C(15)	2.241(8)	Ir–C(21)	1.931(8)
S(1)–C(1)	1.754(7)	S(2)–C(2)	1.737(8)
N(3)–C(3)	1.13(1)	N(4)–C(4)	1.14(1)
N(21)–C(21)	1.14(1)	N(21)–C(22)	1.45(1)
C(1)–C(2)	1.35(1)	C(1)–C(3)	1.44(1)
C(2)–C(4)	1.43(1)	C(11)–C(12)	1.45(1)
C(11)–C(15)	1.45(1)	C(12)–C(13)	1.41(1)
C(13)–C(14)	1.45(1)	C(14)–C(15)	1.40(1)
Ir–Cp^* (centroid)	1.88(1)		
Bond angles			
S(1)–Ir–S(2)	88.20(7)	S(1)–Ir–C(21)	89.9(2)
S(2)–Ir–C(21)	92.8(3)	Ir–S(1)–C(1)	101.9(2)
Ir–S(2)–C(2)	102.4(3)	C(21)–N(21)–C(22)	177.7(8)
S(1)–C(1)–C(2)	123.4(6)	S(1)–C(1)–C(3)	116.8(5)
C(2)–C(1)–C(3)	119.8(7)	S(2)–C(2)–C(1)	123.3(6)
S(2)–C(2)–C(4)	116.9(5)	C(1)–C(2)–C(4)	119.7(7)
N(3)–C(3)–C(1)	178.1(9)	N(4)–C(4)–C(2)	179.0(8)
Ir–C(21)–N(21)	175.9(8)		

[a] Numbers in parentheses are estimated standard deviations in the least significant digits

Table 5
Cyclic voltammetric data for compounds **1–3** [a]

Compound	Redox couple [b]								
	0/+1				+1/+2				0/−1 [c]
	E_{p^a}	E_{p^c}	i_{p^c}/i_{p^a}	$E_{1/2}$	E_{p^a}	E_{p^c}	i_{p^c}/i_{p^a}	$E_{1/2}$	E_{p^c}
1 (MeCN)	0.51	0.43	1.0	0.47	1.23	1.15	0.90	1.19	−2.21 [d]
1 (CH_2Cl_2)	0.54	0.46	1.0	0.50	1.23	[c]	–	–	
2 (MeCN)	0.50	0.43	1.0	0.47	1.26	1.19	0.91	1.23	−2.11 [d]
2 (CH_2Cl_2)	0.60	0.53	1.0	0.57	1.39	[c]	–	–	
3 (MeCN) [e]	0.56	0.48	1.0	0.52	1.21	[c]	–	–	−2.00 [d]
3 (CH_2Cl_2) [f]	0.62	0.54	1.0	0.58	1.25	[c]	–	–	

[a] All cyclic voltammograms were recorded at room temperature in solutions containing 0.2 M TBAP at a scan rate of 0.5 V s^{-1}. Potentials are in volts relative to a silver wire quasi-reference electrode calibrated against added $[Cp_2Co][PF_6]$
[b] E_{p^a} and E_{p^c} refer to the anodic and cathodic peak potentials for a given redox couple
[c] No reverse redox couple was observed
[d] Reduction wave outside the solvent window
[e] An additional redox response at $E_{p^a} = 1.34$ V was observed
[f] An additional redox response at $E_{p^a} = 1.39$ V was observed

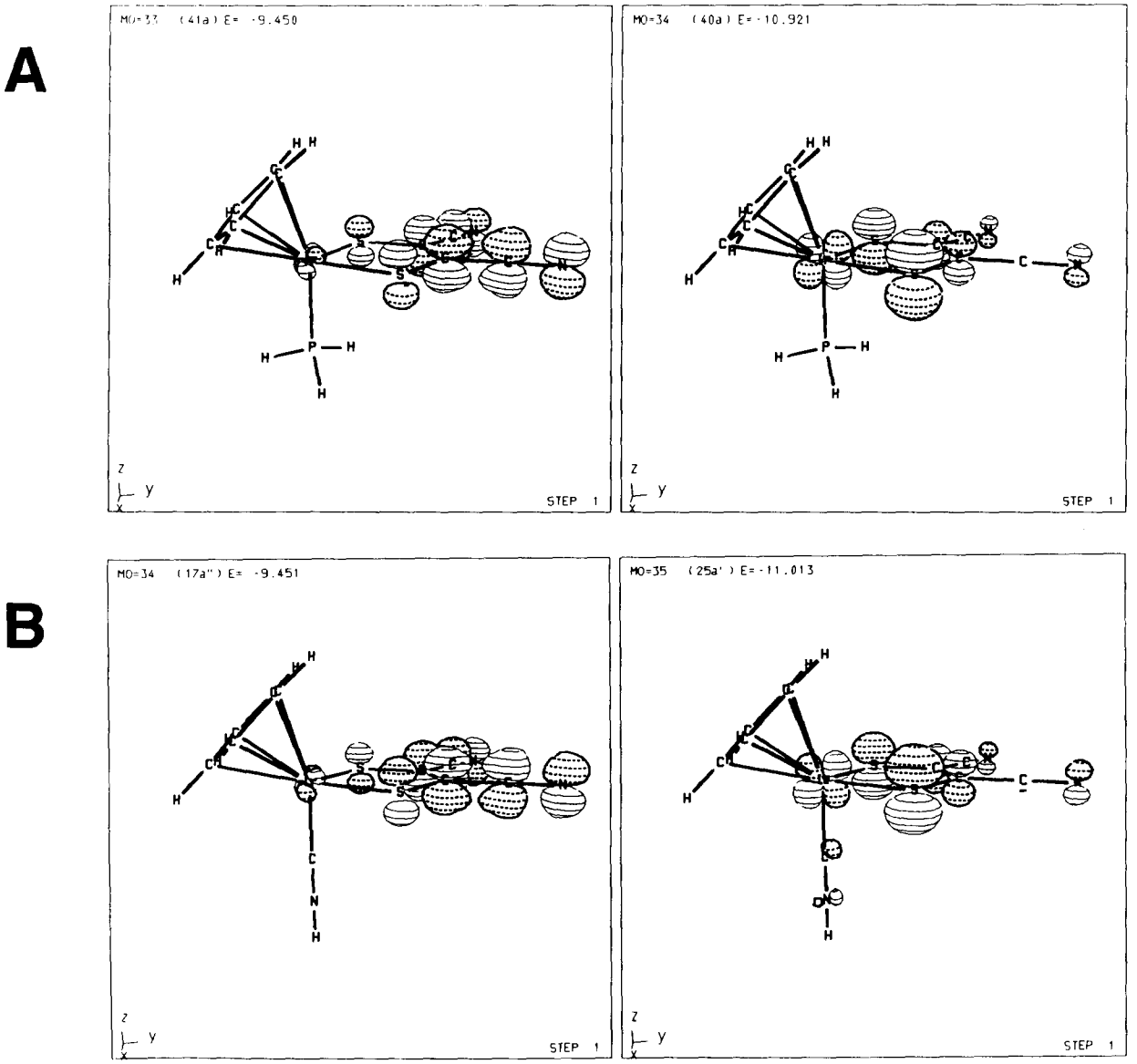

Fig. 3. CACAO drawings of the LUMO (left side) and the HOMO (right side) of (a) $CpIr(PH_3)(mnt)$ and (b) CpIr(CNH)(mnt).

stability of the $+1/+2$ redox couple in **3**. This trend is consistent with a greater destabilization of the $+1/+2$ redox couple by the ancillary isonitrile ligand, as it is known that isonitriles are stronger π acceptors relative to alkyl- and arylphosphines [27].

Compounds **1–3** all reveal the presence of an irreversible reduction wave in MeCN solvent at ca. -2.1 V (see Table 5). The reduction remained irreversible under a variety of conditions (i.e. fast scan rates and reduced temperatures) and was not examined further.

The electron stoichiometry associated with the $0/+1$ redox couple was also explored at a platinum electrode by rotating disc voltammetry (RDE) in MeCN solvent containing 0.25 M TBAP. In each case, the half-wave potential obtained from the RDE experiment agreed well with the data obtained from cyclic voltammetry. Nernstian behaviour was observed for all of the $0/+1$ redox couples in **1–3**, on the basis of the data obtained from plots of E vs. $\log[(i_d - i)/i]$. Such plots afforded slopes of the order of 60 mV, consistent with a reversible one-electron transfer. Treatment of the same RDE data using Tomes' reversibility criterion ($|E_{3/4} - E_{1/4}|$) gave values of 60–65 mV for **1–3** [28], in excellent agreement with the potential/current plots. The RDE for **1** is shown in Fig. 2(c), where near identical limiting currents (i_d) are seen for both oxidation couples.

2.4. Extended Hückel molecular orbital calculations

The orbital composition of the HOMO and LUMO in **1–3** was established by extended Hückel molecular orbital calculations, using the model phosphine and isonitrile compounds $CpIr(PH_3)(mnt)$ and $CpIr(CNH)(mnt)$. Fig. 3 shows the three-dimensional CACAO drawings of these orbitals along with their respective energies [29].

The HOMO in each compound may be described as being derived from an out-of-phase overlap of iridium dyz (30%) and sulphur (38%) pz orbitals. This type of orbital interaction (i.e. filled–filled π interaction) has been previously observed and discussed by Enemark for the dithiol complex $CpMo(NO)(SH)_2$ [30]. The qualitative molecular orbital diagram in Fig. 4, which was constructed from the known fragment $[Cp^*IrL]^{2+}$ and mnt^{2-} [31], illustrates this interaction and shows selected interactions of the important valence orbitals of each fragment. Clearly observed in the MO diagram is the two-below-one pattern from the remnant t_{2g} orbitals that gives the $d\pi$ orbitals (dxz and dyz) involved in iridium $d\pi$-sulphur $p\pi$ overlap [30]. The MO diagram reveals that the LUMO in $Cp^*Ir(PH_3)(mnt)$ and $Cp^*Ir(CNH)(mnt)$ is composed of an overlap of pz orbitals derived from the mnt ligand (98%), with a minor contribution from the iridium dxz orbital. The metal–sulphur overlap in the LUMO is antibonding,

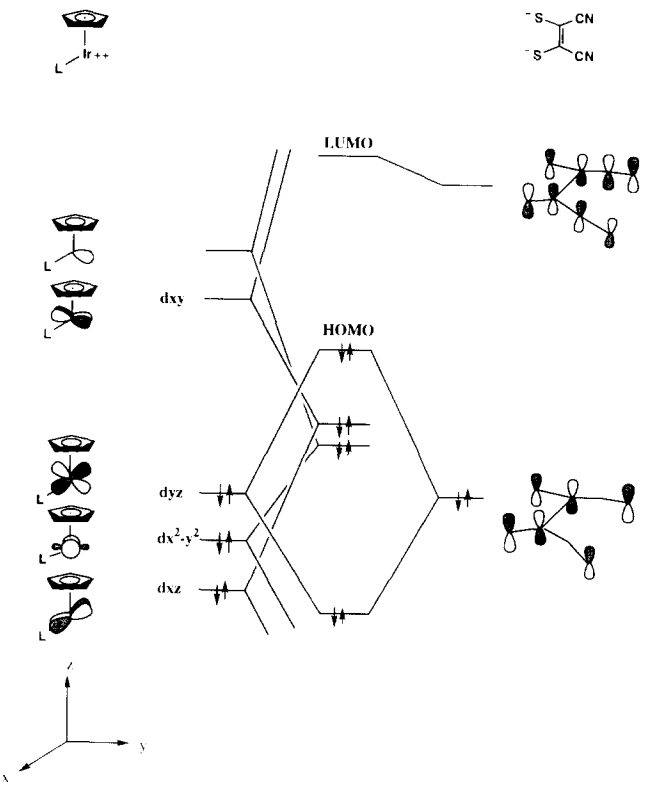

Fig. 4. Qualitative molecular orbital diagram for CpIr(L)(mnt) showing selected valence orbital interactions.

with the mnt π level being slightly destabilized by the lower-lying metal orbitals.

3. Conclusions

The mnt-substituted iridium complexes $Cp^*Ir(L)(mnt)$ have been synthesized and characterized in solution by IR and NMR spectroscopies and by X-ray crystallography in the case of the PPh_3 and CN-t-Bu derivatives. The electrochemical properties of **1–3** have been examined by cyclic and rotating disc electrode voltammetric techniques. Extended Hückel MO data have allowed for the determination of the HOMO and LUMO in these complexes.

4. Experimental section

The starting materials disodium maleonitriledithiolate [21] and the cyclopentadienyl complexes $Cp^*Ir(L)Cl_2$ [20] were prepared by using known literature procedures. The EtOH employed in the synthesis of **1–3** was degassed immediately before use with argon. The tetra-n-butylammonium perchlorate (*caution: strong oxidant*) used in the CV and RDE studies was purchased from Johnson Matthey Electronics and recrystallized from ethyl acetate/petroleum ether, after which it dried un-

der vacuum for 2 days. The microanalyses were performed by Atlantic Microlab, Atlanta, GA.

All infrared spectra were recorded on a Nicolet 20 SXB FT-IR spectrometer in 0.1 mm NaCl cells. The ^{1}H and ^{13}C NMR spectra were recorded on a Varian 200 VXR spectrometer at 200 and 50 MHz, respectively.

4.1. Synthesis of $Cp^*Ir(PMe_3)(mnt)$

Since all of the procedures were carried out in an identical fashion, only the synthesis for $Cp^*Ir(PMe_3)$(mnt) will be described in detail. To 0.10 g (0.21 mmol) of $Cp^*Ir(PMe_3)Cl_2$ and 43.0 mg (0.23 mmol) of Na_2mnt in a Schlenk tube was added degassed EtOH (ca. 50 ml), after which the reaction was heated for several hours at 45°C. TLC analysis using CH_2Cl_2 as the eluent revealed a slow-moving spot having an R_f value of 0.27. This material was next isolated by preparative column chromatography over silica gel using the same solvent as the TLC. Recrystallization of the crude product from CH_2Cl_2/pentane afforded analytically pure **1** as a red solid. Yield: 0.09 g (79%). IR (CH_2Cl_2): 2211 (m, CN), 2200 (s, CN) cm^{-1}. Anal. Found C, 37.46; H, 4.40. $C_{17}H_{24}IrN_2PS_2$ calcd: C, 37.55; H, 4.45.

4.2. $Cp^*Ir(PPh_3)(mnt)$

The sample was isolated in manner as described above for **1**, and recrystallization from CH_2Cl_2/pentane afforded the analytical sample and single crystals of **2** suitable for X-ray diffraction analysis. Yield: 0.13 g (85%). IR (CH_2Cl_2): 2212 (m, CN), 2200 (s, CN) cm^{-1}. Anal. Found C, 52.43; H, 4.09. $C_{32}H_{30}IrN_2PS_2$ calcd: C, 52.66; H, 4.14.

4.3. $Cp^*Ir(CN\text{-}t\text{-}Bu)(mnt)$

The sample was isolated in an analogous fashion and recrystallized from CH_2Cl_2/pentane, which gave analytically pure **3** and crystals suitable for X-ray diffraction analysis. Yield: 0.09 g (78%). IR (CH_2Cl_2): 2212 (m, CN), 2201 (s, CN), 2179 (vs, CN-t-Bu) cm^{-1}. Anal. Found C, 41.39; H, 4.32. $C_{19}H_{24}IrN_3S_2$ calcd: C, 41.42; H, 4.36.

4.4. X-ray diffraction structure for $Cp^*Ir(PPh_3)(mnt)$

A purple crystal of dimensions $0.08 \times 0.42 \times 0.57$ mm^3 was sealed inside a Lindemann capillary and then mounted on an Enraf-Nonius CAD-4 diffractometer. Cell constants were obtained from a least-squares refinement of 25 reflections with $2\theta > 36°$. Intensity data in the range $2.0 \leqslant 2\theta \leqslant 44°$ were collected at room temperature using the $\theta/2\theta$ scan technique in the variable-scan mode and were corrected for Lorentz, polarization and absorption (DIFABS). Three reflections (800, 080, 004) were measured after every 3600 s of exposure time in order to monitor crystal decay ($< 1\%$). The structure was solved by using standard Patterson techniques, which revealed the position of the iridium atom. All remaining non-hydrogen atoms were located with difference Fourier maps and full-matrix least-squares refinement and refined anisotropically. Refinement converged at $R = 0.0281$ and $R_w = 0.0318$ for 3425 unique reflections with $I > 3\sigma(I)$.

4.5. X-ray diffraction structure for $Cp^*Ir(CN\text{-}t\text{-}Bu)(mnt)$

A red crystal of $Cp^*Ir(CN\text{-}t\text{-}Bu)(mnt)$ of dimensions $0.05 \times 0.22 \times 0.54$ mm^3 was prepared as discussed for **2**. Cell constants were obtained from a least-squares refinement of 25 reflections with $2\theta > 40°$. Intensity data in the range $2.0 \leqslant 2\theta \leqslant 44°$ were collected at room temperature using the ω scan technique in the variable-scan speed mode and were collected for Lorentz, polarization and absorption (DIFABS). Three reflections (600, 0140, 008) were measured after every 3600 s of exposure time in order to monitor crystal decay ($< 1\%$). The structure was solved by using standard Patterson techniques, which revealed the position of the iridium atom. All remaining non-hydrogen atoms were located with difference Fourier maps and full-matrix least-squares refinement. With the exception of the t-butyl carbons, all non-hydrogen atoms were refined anisotropically. Refinement converged at $R = 0.0245$ and $R_w = 0.0279$ for 2266 unique reflections with $I > 3\sigma(I)$.

4.6. Electrochemical studies

Cyclic and rotating disc electrode voltammograms were obtained with a PAR Model 273 potentiostat/galvanostat, equipped with positive feedback circuitry to compensate for IR drop. The cell used in the CV studies was of airtight design and based on a three-electrode configuration. All CV experiments employed a platinum disc (area = 0.0079 cm^2) as the working and auxiliary electrode. The RDE studies were recorded in a Vacuum Atmospheres Dribox at room temperature using a PAR Model 616 RDE unit. The working electrode consisted of a commercially available platinum disc electrode (area = 0.126 cm^2). All voltammograms (CV and RDE) utilized a silver wire quasi-reference electrode, and all potential data are referenced relative to the formal potential of the Cp_2Co^+/Cp_2Co (internally added) redox couple, taken to have $E_{1/2} = -1.00$ V [32].

4.7. Extended Hückel molecular orbital calculations

The extended Hückel calculations reported here were carried out with the original program developed by

Hoffmann [33], as modified by Mealli and Proserpio [29].

5. Supplementary material available

Listings of observed and calculated structure factor amplitudes, tables of anisotropic thermal parameters, and idealized hydrogen parameters. Ordering information can be supplied by the authors upon request.

Acknowledgements

We are grateful to the Engelhard Corporation for providing us with the $IrCl_3 \cdot 3H_2O$ used in the preparation of compounds **1–3** and to Professor Carlo Mealli for providing us with a copy of his CACAO drawing program. Financial support from the Robert A. Welch Foundation (B-1202-SGB and B-1039-MGR) and the UNT Faculty Research Program is appreciated.

References

[1] G.N. Schrauzer, *Acc. Chem. Res., 2* (1969) 72.
[2] R.P. Burns and C.A. McAuliffe, *Adv. Inorg. Chem. Radiochem., 22* (1979) 303.
[3] J.A. McCleverty, *Prog. Inorg. Chem., 10* (1968) 49.
[4] S.P. Best, S.A. Ciniawsky, R.J.H. Clark and R.C.S. McQueen, *J. Chem. Soc., Dalton Trans.* (1993) 2267.
[5] J.A. McCleverty, N.M. Atherton, J. Locke, E.J. Wharton and C.J. Winscom, *J. Am. Chem. Soc., 89* (1967) 6082.
[6] T.R. Miller and I.G. Dance, *J. Am. Chem. Soc., 95* (1973) 6970.
[7] (a) V. Gama, R.T. Henriques, G. Bonfait, L.C. Pereira, J.C. Waerenborgh, I.C. Santos, M.T. Duarte, J.M.P. Cabral and M. Almeida, *Inorg. Chem., 31* (1992) 2598, and references therein; (b) V. Gama, R.T. Henriques, M. Almeida, L. Veiros, M.J. Calhorda, A. Meetsma and J.L. de Boer, *Inorg. Chem., 32* (1993) 3705.
[8] For electron transfer and luminescent reactivity, see: (a) A. Vogler and H. Kunkely, *J. Chem. Soc., Chem. Commun.* (1986) 1616; (b) H. Kisch, W. Dumler, C. Chiorboli, F. Scandola, J. Salbeck and J. Daub, *J. Phys. Chem., 96* (1992) 10323; (c) P. Bradley, C.E. Johnson and R. Eisenberg, *J. Chem. Soc., Chem. Commun.* (1988) 255; (d) C.E. Johnson, R. Eisenberg, T.R. Evans and M.S. Burberry, *J. Am. Chem. Soc., 105* (1983) 1795; (e) E.G. Megehee, C.E. Johnson and R. Eisenberg, *Inorg. Chem., 28* (1989) 2423; (f) J.A. Zuleta, M.S. Burberry and R. Eisenberg, *Coord. Chem. Rev., 97* (1990) 47; (g) J.A. Zuleta, J.M. Bevilacqua, J.M. Rehm and R. Eisenberg, *Inorg. Chem., 31* (1992) 1332; (h) J.A. Zuleta, J.M. Bevilacqua, D.M. Proserpio, P.D. Harvey and R. Eisenberg, *Inorg. Chem., 31* (1992) 2396; (i) J.M. Bevilacqua, J.A. Zuleta and R. Eisenberq, *Inorg. Chem., 32* (1993) 3689.
[9] M.R. Churchill and J.P. Fennessey, *Inorg. Chem., 7* (1968) 1123.
[10] P. Hydes, J.A. McCleverty and D.G. Orchard, *J. Chem. Soc. (A)* (1971) 3660.
[11] J.A. McCleverty and D.G. Orchard, *J. Chem. Soc. (A)* (1970) 3315.
[12] J.A. McCleverty, T.A. James and E.J. Wharton, *Inorg. Chem., 6* (1969) 1340.
[13] T.A. James and J.A. McCleverty, *J. Chem. Soc. (A)* (1970) 3308.
[14] J. Locke and J.A. McCleverty, *Inorg. Chem., 5* (1966) 1157.
[15] M. Sakurada, M. Kajitani, H. Hatano, Y. Matsudaira, T. Suetsugu, S. Ono, T. Akiyama and A. Sugimori, *Organometallics, 11* (1992) 2337.
[16] S.D. Henderson, T.A. Stephenson and E.J. Wharton, *J. Organomet. Chem., 179* (1979) 43.
[17] R. Ziessel, M.-T. Youinou, F. Balegroune and D. Grandjean, *J. Organomet. Chem., 441* (1992) 143.
[18] K. Yang, S.G. Bott and M.G. Richmond, *J. Organomet. Chem., 483* (1994) 7.
[19] C.-G. Xia, S.G. Bott and M.G. Richmond, *Inorg. Chim. Acta, 226* (1994) 267.
[20] (a) J.W. Kang, K. Moseley and P.M. Maitlis, *J. Am. Chem. Soc., 91* (1969) 5970; (b) K. Moseley, J.W. Kang and P.M. Maitlis, *J. Chem. Soc. (A)* (1970) 2875; (c) K. Isobe, P.M. Bailey and P.M. Maitlis, *J. Chem. Soc., Dalton Trans.* (1981) 2003; (d) B.L. Booth, R.N. Haszeldine and M. Hill, *J. Organomet. Chem., 16* (1969) 491; (e) M. Herberhold, G.-X. Jin, A.L. Rheingold and G.F. Sheats, *Z. Naturforsch., 47b* (1992) 1091.
[21] A. Davison and R.H. Holm, *Inorg. Synth., 10* (1967) 8.
[22] (a) D.G.I. Felton and S.F.D. Orr, *J. Chem. Soc.* (1955) 2170; (b) D. Dolphin and A. Wick, *Tabulation of Infrared Spectral Data*, Wiley-Interscience, New York, 1977.
[23] G.C. Levy and G.L. Nelson, *Carbon-13 Nuclear Magnetic Resonance for Organic Chemists*, Wiley-Interscience, New York, 1972.
[24] (a) G.P. Khare and R. Eisenberg, *Inorg. Chem., 11* (1972) 1385; (b) R. Kramer, K. Polborn and W. Beck, *J. Organomet. Chem., 410* (1991) 111; (c) J. Chen, L.M. Daniels and R.J. Angelici, *J. Am. Chem. Soc., 113* (1991) 2544; (d) D.P. Klein, G.M. Kloster and R.G. Bergman, *J. Am. Chem. Soc., 112* (1990) 2022.
[25] (a) W.D. Jones, R.P. Duttweiler Jr and F.J. Feher, *Inorg. Chem., 29* (1990) 1505; (b) T. Pill, K. Polborn and W. Beck, *Chem. Ber., 123* (1990) 11.
[26] (a) A.J. Bard and L.R. Faulkner, *Electrochemical Methods*, Wiley, New York, 1980; (b) P.H. Rieger, *Electrochemistry*, Chapman & Hall, New York, 1994.
[27] C.M. Lukehart, *Fundamental Transition Metal Organometallic Chemistry*, Brooks/Cole Publishing Co., Monterey CA, 1985.
[28] J. Tomes, *Coll. Czech. Chem. Commun., 9* (1937) 12, 81, 150.
[29] C. Mealli and D.M. Proserpio, *J. Chem. Ed., 67* (1990) 399.
[30] (a) M.T. Ashby and J.H. Enemark, *J. Am. Chem. Soc., 108* (1986) 730; (b) A.D. Hunter, P. Legzdins, F.W.B. Einstein, A.C. Willis, B.E. Bursten and M.G. Gatter, *J. Am. Chem. Soc., 108* (1986) 3843.
[31] For the orbital properties of the d^8-ML_4 fragment, see: (a) P. Hofmann, *Angew. Chem., Int. Ed. Engl., 18* (1979) 554; (b) P. Hofmann and M. Padmanabhan, *Organometallics, 2* (1983) 1273; (c) J.-Y. Saillard and R. Hoffmann, *J. Am. Chem. Soc., 106* (1984) 2006; (d) J. Silvestre, M.J. Calhorda, R. Hoffmann, P.O. Stoutland and R.G. Bergman, *Organometallics, 5* (1986) 1841.
[32] W.E. Geiger Jr, *J. Am. Chem. Soc., 96* (1974) 2632.
[33] (a) R. Hoffmann, *J. Chem. Phys., 39* (1963) 1397; (b) R. Hoffmann and W.N. Libscomb, *J. Chem. Phys., 36* (1962) 3179.